International Journal of Refrigeration 93 (2018) 259–268

Contents lists available at ScienceDirect

International Journal of Refrigeration

journal homepage: www.elsevier.com/locate/ijrefrig

Condensation heat transfer of R134a, R1234ze(E) and R290 on horizontal plain and enhanced titanium tubes

Wen-Tao Ji[a,*], Guo-Hun Chong[a], Chuang-Yao Zhao[a], Hu Zhang[b], Wen-Quan Tao[a]

[a] Key Laboratory of Thermo-Fluid Science and Engineering of MOE, School of Energy and Power Engineering, Xi'an Jiaotong University, Xi'an 710049, China
[b] State Key Laboratory for Strength and Vibration of Mechanical Structures, Xi'an Jiaotong University, Xi'an 710049, China

ARTICLE INFO

Article history:
Received 7 February 2018
Revised 2 May 2018
Accepted 23 June 2018
Available online 3 July 2018

Keywords:
Condensation
Heat transfer
Refrigerant
Tube

ABSTRACT

An experimental investigation on the condensation of R134a, R1234ze(E) and R290 outside plain and enhanced titanium tubes was conducted. The saturation temperature in the experiments was 35 °C to 40 °C, and heat flux was in the range of 8–80 kW/m^2. Effects of heat flux, refrigerant and saturation temperature on heat transfer were investigated. The heat transfer enhancement ratio of overall heat transfer coefficient decreased with increasing heat flux. It was found that the condensing heat transfer coefficient of R134a, compared with R1234ze(E) and R290, was the largest for plain and enhanced tubes. Saturation temperature had minor effect on condensing heat transfer coefficient for R134a, R1234ze(E) and R290 for plain tube. The effect of saturate temperature on the condensing heat transfer of R134a and R1234ze(E) was even negligible for enhanced tube. While, the condensing heat transfer coefficient of R290 for enhanced tube was increasing with increment of saturation temperature. Experimental condensing heat transfer coefficient were also compared with five predicting models for low-fin tube. It showed that the model of Briggs–Rose gave a better prediction result for R134a and R1234ze(E), while the model underestimated the experimental result for R290.

Transfert de chaleur par condensation de R134a, R1234ze(E) et R290 sur des tubes horizontaux en titane simples et améliorés

Mots-clés: Condensation; Transfert de chaleur; Frigorigène; Tube

1. Introduction

Condensation is a very efficient heat transfer mode in air conditioning and refrigeration. The common methods for improving condensation transfer performance can be broadly separated into two aspects: decreasing the film thickness outside the fin and using refrigerant with higher heat transfer performance. A continuous demand for efficiency still urges the studies on condensation of refrigerants over horizontal enhanced tubes, such as the effects of fin density, height of fin, material, surface structure, and so on (Al-Badri et al., 2016; Ji et al., 2014, 2015a, 2015b; Zhao et al., 2017).

Recently, Al-Badri et al. (2016) investigated the influence of fin structure and fin density on the condensation heat transfer of R134a for single finned tubes and tube bundles. Experimental results showed that condensing heat transfer coefficients of three dimensional enhanced tube were apparently higher than standard low-fin tubes at same wall subcooling. In addition, experimental results for single tube were also compared with analytical prediction models of Briggs and Rose (1994) and Al-Badri et al. (2013). It indicated that experimental results were overestimated by Al-Badri model, whereas Briggs and Rose underestimated the results.

Condensation heat transfer on horizontal single plain tube for R1234ze(E), R1234ze(Z), and R1233zd(E) was studied by Nagata et al. (2016). Condensing heat transfer coefficients of R1234ze(E), R1234ze(Z), and R1233zd(E) were measured at different saturation temperature. It was found that condensing heat transfer coefficient of R1234ze(E) was about 8% lower than R134a at saturation tem-

* Corresponding author.
E-mail address: wentaoji@xjtu.edu.cn (W.-T. Ji).

https://doi.org/10.1016/j.ijrefrig.2018.06.013
0140-7007/

Nomenclature

A	area [m^2]
c_p	specific heat capacity [J kg^{-1} K^{-1}]
d	diameter of tube [mm]
e	height of outside fin [mm]
f	drag coefficient
g	gravitational acceleration [m s^{-2}]
h	heat transfer coefficients [W m^{-2} K^{-1}]
k	overall heat transfer coefficients [W m^{-2} K^{-1}]
L	tube's test length [m]
m	mass flow rate [kg s^{-1}]
Pr	Prandtl number in Gnielinski equation
q	heat flux [W m^{-2}]
Re	Reynolds number
R_f	thermal resistance of foul [m^2 K W^{-1}]
R_w	thermal resistance of tube wall [m^2 K W^{-1}]
t	temperature [°C]

Greek symbols

ϕ	heat transfer rate [W]
λ	thermal conductivity [W m^{-1} K^{-1}]
η	viscosity [Pa s]
ρ	density [kg m^{-3}]
r	latent heat [kJ kg^{-1}]
σ	surface tension [mN m]
Δt_m	logarithmic mean temperature difference [K]

Subscripts

b	boiling
c	condensing
i	inside of tube
in	inlet of tube
ip	inside of plain tube
l	liquid
o	outside of tube
out	outlet of tube
p	plain
s	saturation
w	wall

perature of 40 °C. The heat transfer coefficient of R1234ze(Z) was approximately 10% higher than R245fa. Condensing heat transfer coefficient of R1233zd(E) was similar with R245fa.

Table 1
Specifications of test tubes.

Tubes	Outside diameter d_o(mm)	Inside diameter d_i(mm)	Thickness of outside fin δ(mm)	Height of outside fin e(mm)	Outside fins per inch
Plain	15.99	14.85	-	-	-
Enhanced	16.01	14.87	0.362	0.300	33

Heat exchangers with copper tubes are widely used in industrial applications. But the copper tube is not suitable for some occasions such as anticorrosion and low weight. Titanium, offers superb properties and could meet the above requirements. It indicated that most studies of on condensation heat transfer of refrigerant are mainly conducted on copper tubes. The studies on condensation heat transfer of refrigerant outside titanium tubes are still quite limited. In this work, condensation heat transfer of R134a, R1234ze(E) and R290 outside plain and enhanced titanium tubes were investigated with an experimental approach.

2. Experimental apparatus

Experimental system shown in Fig. 1 consists of three cycles, refrigerants, cooling and heating water. Two titanium tubes, a plain tube and an enhanced tube, are fixed in the condenser at the position over liquid level. Also one copper tube, called boiling tube, is fixed at near bottom of condenser, which is used to heat liquid refrigerant and generate vapor. Cooling water flows through the inside of test tube, and returns to the cold water tank. The temperature can be adjusted in the range of 1–40 °C. Heating water circulation are similar with cooling water, which can provide the temperature ranging from 30 °C to 50 °C.

There is a pressure gauge installed at condenser with precision of 0.01% FS to measure the pressure. The flow rates are measured with electromagnetic flow meters (Error is within 0.1% in the whole measurement range). As shown in Fig. 1, seven RTD probes (PT100) are used to measure the temperature in the system with the precision of ±0.05 °C. They are mounted at the inlet and the outlet of heating and cooling water to obtain the temperature of water flow. Three probes are fixed in the condenser to measure the temperatures of refrigerant vapor and liquid.

The specific geometric parameters of testing plain and enhanced tubes are shown in Table 1. The structure of enhanced tube is shown in Fig. 2.

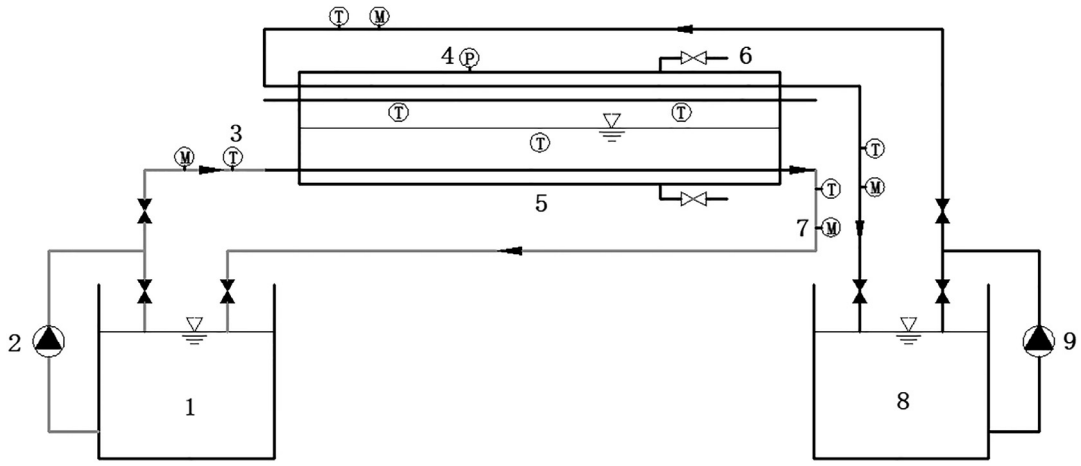

Fig. 1. Schematic diagram of the experimental apparatus. (1) Hot water storage tank (2) Heating water pump (3) Platinum resistance thermometer (4) Pressure gauge (5) Condenser (6) Exhausting valve (7) Flow meter (8) Coldwater storage tank (9) Cooling water pump.

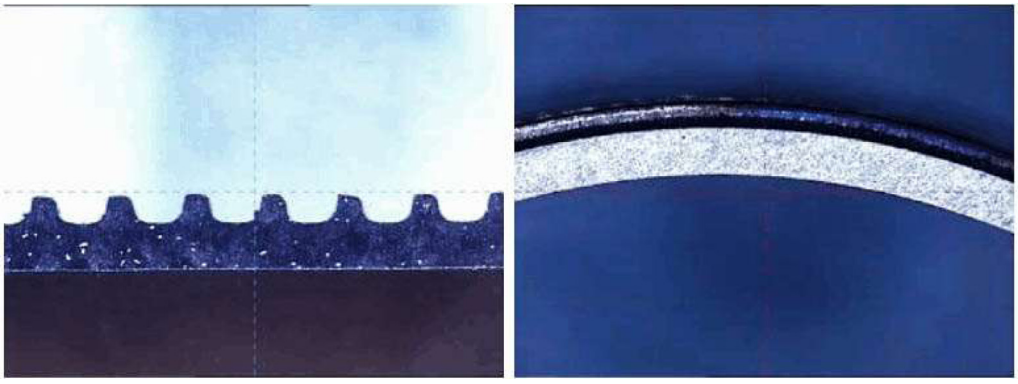

Fig. 2. Geometric structure of enhanced titanium tube.

3. Experimental procedures

After the tubes were fixed in condenser, high pressure nitrogen was charged into the condenser. Tightness check was conducted to ensure the condenser being fully sealed. A vacuum pump was used to evacuate the condenser to a pressure lower than 800 Pa. Finally, liquid refrigerant was charged into the system till the liquid level above the tubes was no less than 20 mm. The experiment was then conducted.

4. Data reduction and uncertainty analysis

The equations to calculate the heat transfer rate of condensation and boiling are as follows.

$$\phi_c = m_c c_p (t_{c,in} - t_{c,out}) \tag{1}$$

$$\phi_b = m_b c_p (t_{b,in} - t_{b,out}) \tag{2}$$

where ϕ_c, ϕ_b are the heat transfer rate (W) in condensation and boiling. $t_{c,\,in}$, $t_{c,\,out}$, respectively, represent the inlet and outlet temperature for cooling water. $t_{b,\,in}$, $t_{b,\,out}$ represent the inlet and outlet temperature for heating water. m_c and m_b are the mass flow rate (kg/s) for cooling and heating water. c_p is the specific heat capacity (J/kg·K) corresponding to the mean temperature of inlet and outlet water. The heat balance for most (90%) experiment data is within ± 3%.

Next, the overall heat transfer coefficient will be calculated by the equation:

$$k = \frac{\phi}{A_o \cdot \Delta t_m} \tag{3}$$

where ϕ, calculating by the average of ϕ_c and ϕ_b, is overall heat transfer rate. A_o is external surface area for the test tube. Δt_m is logarithmic mean temperature difference, which can be calculated as follows.

$$\Delta t_m = \frac{t_{c,in} - t_{c,out}}{\ln \frac{t_s - t_{c,out}}{t_s - t_{c,in}}} \tag{4}$$

where t_s is saturation temperature for the refrigerant in condenser.

Heat flux can be determined by the following equation.

$$q = \frac{\phi}{A_o} \tag{5}$$

Shell-side condensation heat transfer coefficient is obtained with thermal resistance separation method. The overall heat transfer coefficient consists of four parts.

$$\frac{1}{k} = \frac{1}{h_o} + R_w + R_f + \frac{1}{h_i} \cdot \frac{A_o}{A_i} \tag{6}$$

Table 2
Deviations between experimental results and Nusselt analytical solution.

	T_s (°C)	*Deviations* (comparing with Nusselt analytical solution)
R134a	35	−1.97–7.60%
	40	1.87–6.87%
R1234ze(E)	35	−7.32–10.39%
	40	−5.73–8.35%
R290	35	−6.24–11.68%
	40	−9.78–7.94%

where h_o, h_i are heat transfer coefficient of the outer and inner test tube. R_w, calculated through $R_w = 0.5 d_o \ln(d_o/d_i)/\lambda$, is the thermal resistance of tube wall. R_f is fouling thermal resistance, which can be neglected in the present investigation because the running time of experiment is less than one month with clean water. A_i is internal surface area of the test tube. Heat transfer coefficient of inner tube h_i can be determined by Gnielinski equation (Gnielinski, 1976). Finally, after k, R_w, R_f, h_i in Eq. (6) were obtained, then the shell side heat coefficient h_o can be determined.

The uncertainties were estimated according to Cheng and Tao (1994), and Kline (1953). The possible uncertainty of q is 3.07%; Δt_m is 1.1%; k is 3.26%. Referring to literature (Bergman, 2011; Gnielinski, 1976; Yunus and Ghajar, 2007), the uncertainty of Gnielinski equation can be regarded as 20%, which means uncertainty of h_i is 20%. In the light of the method in references (Ji et al., 2014; Lienhard, 2013), the uncertainty of condensing heat transfer coefficient h_o is in the range of 16.74–23.26%.

5. Results and discussion

5.1. Reliability verification of experimental system

In order to check the reliability of experimental system, comparisons between condensation experimental results and Nusselt analytical solution (Nusselt, 1916) on plain tube for R134a, R1234ze(E) and R290 are presented. Nusselt analytical solution is written as:

$$h_o = 0.729\left(\frac{r g \lambda_l^3 \rho_l^2}{\eta_l d_o (t_s - t_w)}\right)^{1/4} = 0.656\left(\frac{r g \lambda_l^3 \rho_l^2}{\eta_l d_o q}\right)^{1/3} \tag{7}$$

Fig. 3 shows the comparisons between condensation experimental results and Nusselt analytical solution for R134a, R1234ze(E) and R290 at the saturation temperature of 35 °C and 40 °C on plain titanium tube. It can be inferred from Table 2 that all deviations were within ± 12% between experimental results and Nusselt analytical solution. The comparison should validate the experimental system and the data reduction procedure.

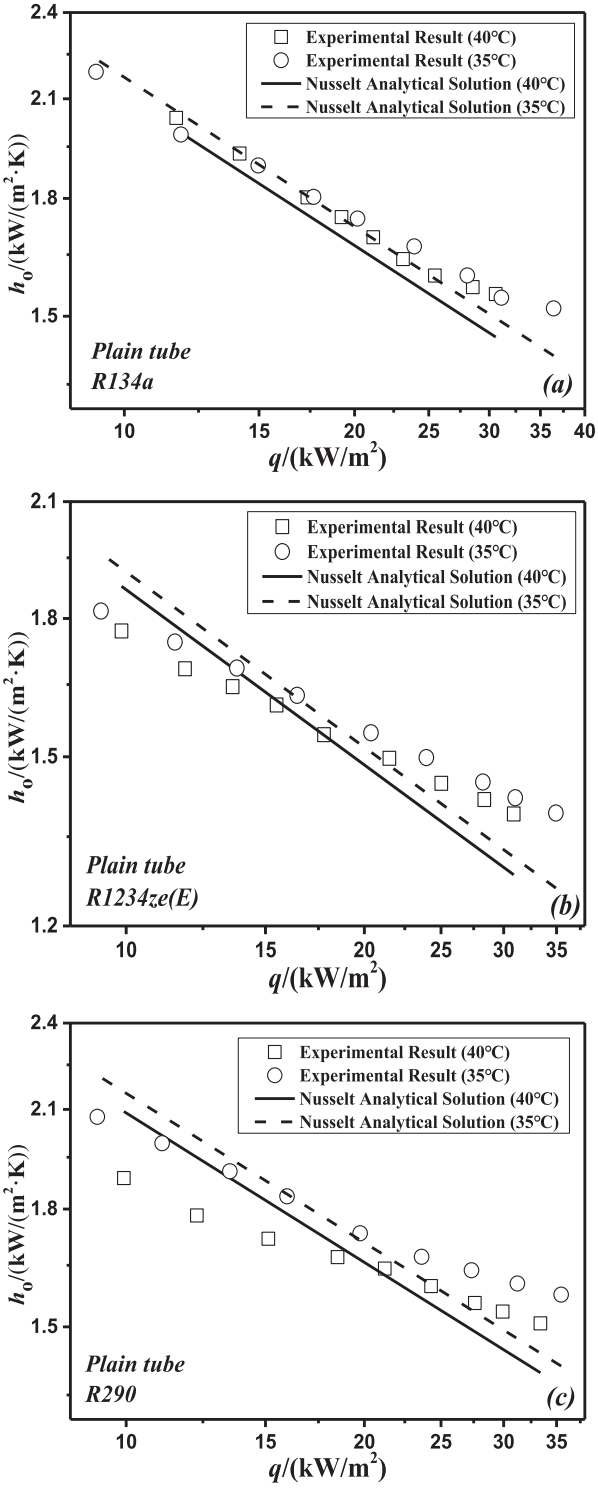

Fig. 3. Comparisons of experimental result with Nusselt analytical solution.

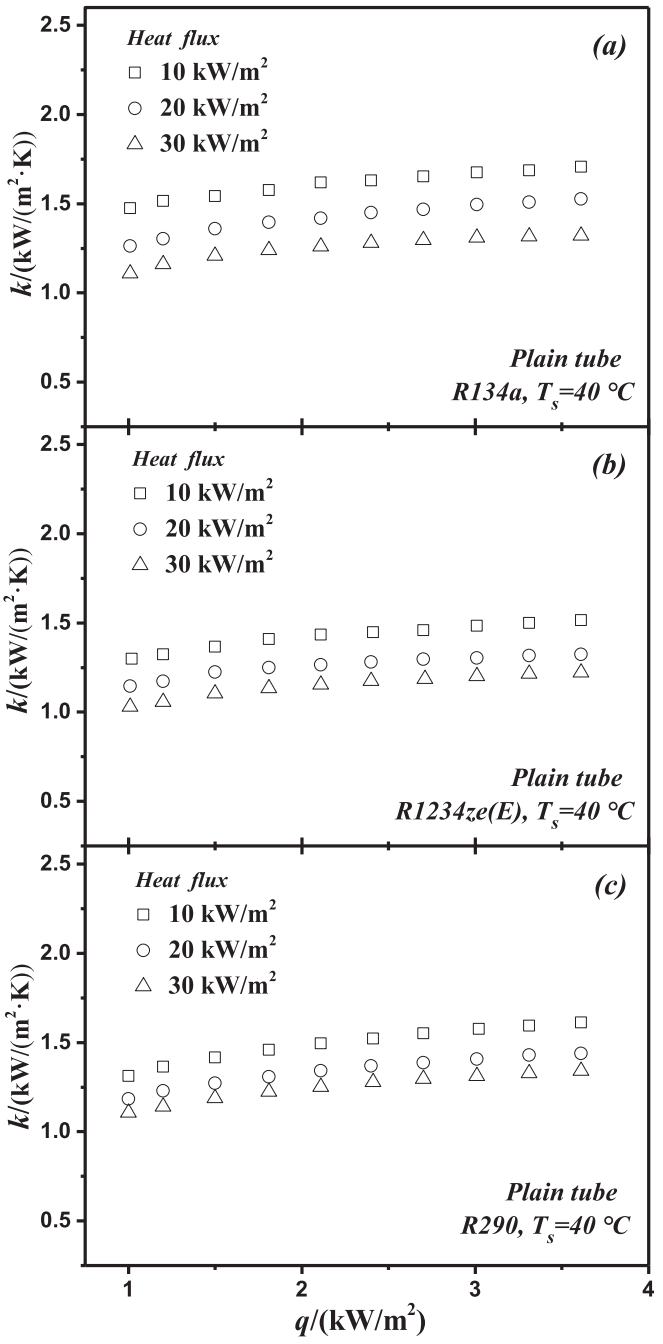

Fig. 4. Overall heat transfer coefficients versus water velocity at different heat flux for plain tube.

5.2. Effect of heat flux on overall heat transfer coefficient

Figs. 4 and 5 show the overall heat transfer coefficients of R134a, R1234ze(E) and R290 versus internal water velocity in different heat flux at saturation temperature of 40 °C for plain and enhanced titanium tubes. For plain tube in Fig. 4 (a) –(c), it is a typical trend that as the increment of internal water velocity, the heat transfer coefficient also increases. The overall heat transfer coefficient of R134a is the largest compared with other two refrigerants.

For enhanced tube in Fig. 5(a)–(c), the typical features are similar with plain tube. Overall heat transfer coefficient increases with increment of internal water velocity. Overall heat transfer coefficient of R134a is 5.87–13.88% higher than R1234ze(E) and 13.39–36.17% higher than R290 at same heat flux. The major difference for R290 is the same increment rate of heat flux corresponding to a rather minor change in overall heat transfer coefficient. The heat transfer coefficient at heat flux of 10 and 20 kW/m^2 was almost the same.

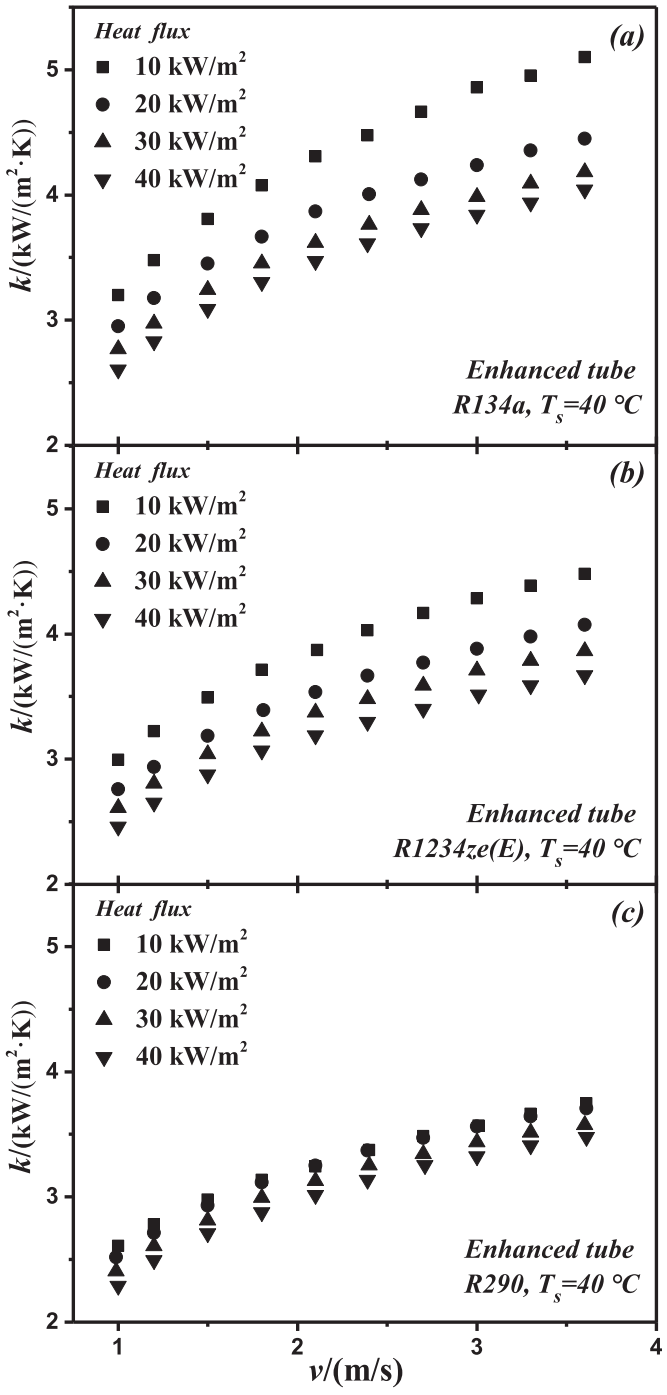

Fig. 5. Overall heat transfer coefficients versus water velocity at different heat flux for enhanced tube.

Comparison of overall heat transfer coefficient for low thermal conductivity plain and enhanced tubes from literature is also presented in Fig. 6. Saturation temperature was 40 °C for all experimental results. Inlet water temperature was 32 °C and 35 °C for enhanced tubes, 25 °C and 32 °C for plain tubes. Materials of tubes included titanium, cupronickel, stainless steel, iron cupronickel, and aluminum brass. Thermal conductivity of tubes was ranging from 15.2 to 104.7 W/(m k) (details could be seen in Table 3). Detailed parameters of tube shape for all tubes are shown in Table 4. As shown in Fig. 6, the overall heat transfer coefficients of stainless steel tubes were the lowest for all materials of plain and enhanced tubes. The reason was that the thermal conductivity for stainless steel was the lowest, and the tube thickness was also relatively thicker comparing with other tube materials. Overall heat transfer coefficients of cupronickel (B10) and aluminum brass (3D fin) enhanced tubes had rather minor difference compared to each other and they are the highest for all tubes in comparison. As shown in Table 3, thermal conductivity of cupronickel (B10) and aluminum brass (3D fin) tubes are higher than other tubes. For cupronickel (B10), the fin density was highest and the structure of aluminum brass (3D fin) is three dimensional. Hence, the overall heat transfer coefficients are higher for the two tubes. It was caused by the combined effect of tube material and structure of fins. The overall heat transfer coefficient was similar for titanium, cupronickel (B30), aluminum brass (2d fin) and iron cupronickel enhanced tubes. As shown in Fig. 6, the overall heat transfer coefficient of titanium plain tube was higher than other plain tubes. It was due to

Table 3
Thermal conductivity of tube materials.

Thermal conductivity	Stainless steel	Titanium	Cupronickel (B30)	Iron cupronickel	Cupronickel (B10)	Aluminum brass
λ (W/m•K)	15.2	22	28.9	28.9	61.5	104.7

Table 4
Detailed parameters of tube shape.

Tubes	Outside diameter (mm)	Inside diameter (mm)	Fin thickness (mm)	Fin height (mm)	Fin pitch (mm)	Fin density (fpi)
Plain titanium (Present work)	15.99	14.85	-	-	-	-
Enhanced titanium (Present work)	16.01	14.87	0.362	0.300	0.784	33
Iron cupronickel (3D) (Zhao et al. 2017)	18.93	16.48	-	-	-	-
Iron cupronickel (2D) (Zhao et al. 2017)	19.25	16.59	0.300	1.290	1.260	21
Aluminum brass (3D) (Zhao et al. 2017)	18.90	15.16	-	-	-	-
Aluminum brass (2D) (Zhao et al. 2017)	19.27	16.58	0.290	1.270	1.240	21
Enhanced titanium (Ji et al. 2014)	19.08	15.94	0.349	0.422	0.686	38
Plain cupronickel (B10) (Ji et al. 2014)	19.00	16.50	-	-	-	-
Enhanced cupronickel (B10) (Ji et al. 2014)	19.15	16.49	0.247	0.678	0.577	45
Plain cupronickel (B30) (Ji et al. 2014)	16.00	11.59	-	-	-	-
Enhanced cupronickel (B30) (Ji et al. 2014)	16.01	11.60	0.404	0.732	0.686	38
Plain stainless steel (Ji et al. 2014)	17.92	14.72	-	-	-	-
Enhanced stainless steel (Ji et al. 2014)	19.00	15.72	0.458	0.868	0.941	28
Enhanced titanium (Fernández-Seara et al., 2010)	19.05	15.85	0.400	0.965	0.800	33
Cu/Ni (1575fpm) (Zhang et al. 2007)	19.18	17.88	-	0.650	0.635	41

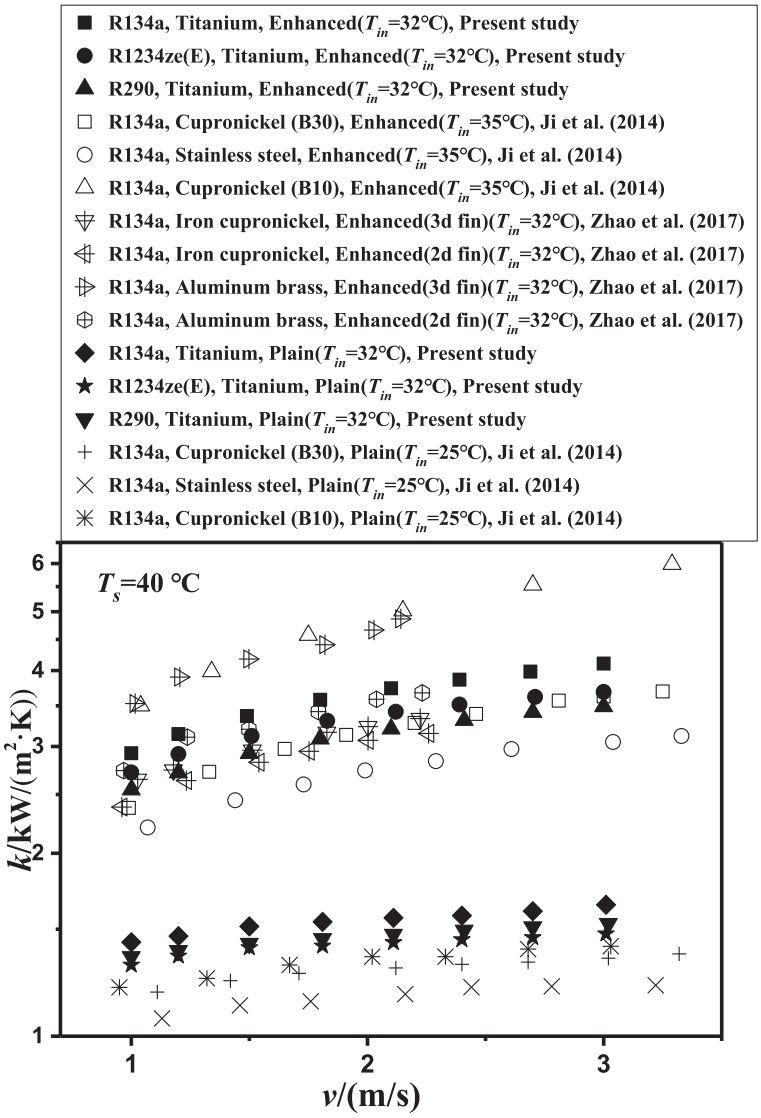

Fig. 6. Comparisons of overall heat transfer coefficients of experimental results for low thermal conductivity tubes.

the testing titanium tube in this paper was the thinnest compared with other tubes, as shown in Table 4.

5.3. Effect of refrigerants on condensing heat transfer coefficient

Fig. 7 presents condensing heat transfer coefficient of R134a, R1234ze(E) and R290 versus heat flux at different saturation temperature for plain and enhanced tubes.

It is observed in Fig. 7 that condensing heat transfer coefficients of R134a, R1234ze(E), and R290 are all decreasing with increment of heat flux. For plain tube in Fig. 7 (a)–(b), most results of condensing heat transfer coefficients show minor difference between R134a and R290. Condensing heat transfer coefficient of R134a is approximately 8.74–17.39% higher than R1234ze(E) at saturation temperature of 40 °C and 8.62–20.21% higher at 35 °C.

Thermophysical properties of R134a, R1234ze(E) and R290 are shown in Table 5. For plain tube, it can be found that heat transfer performance of R134a is similar with R290. R1234ze(E) is relatively lower. As shown in Fig. 7 (c)–(d) for enhanced tube, condensing heat transfer coefficient of R134a is the largest. R290 is the lowest and R1234ze(E) behaves somewhat in between. The major difference for R290 is the surface tension, density and viscosity are all less than R134a and R1234ze(E). Especially the viscosity and density, they are both only one half of the other two refrigerants in the study. At the saturate temperature of 40 °C, surface tension of R290 is 5.0918 mN/m, while, it is 6.1149 and 6.956 for R134a and R1234ze(E). Thus the "Gregorig effect" on enhanced tube for R290 should be less than the other two refrigerants. It might be the reason that R290 has comparable heat transfer coefficient with R134a for plain tube, but the heat transfer coefficient is much lower for enhanced tube. Similar results were also observed in the investigations of Jung et al. (2004) and Gebauer et al. (2013). The condensation heat transfer coefficient of R134a and R290 outside plain tube were almost identical, while the condensing heat transfer outside standard low-fin tube was much lower for R290 than R134a. It indicates that the refrigerant with lower surface tension might have lower heat transfer coefficient for enhanced tube.

For the plain tube at lower heat flux, the condensing heat transfer coefficient of R290 is lower than R134a. While, at higher heat flux more than 30 kW/m^2, it is even higher than R134a. It might be caused by the combined effect of latent heat and surface tension. For the enhanced tube, at higher heat flux more than 60 kW/m^2, it is found that the condensing heat transfer coefficient of all the refrigerant approaches more closely.

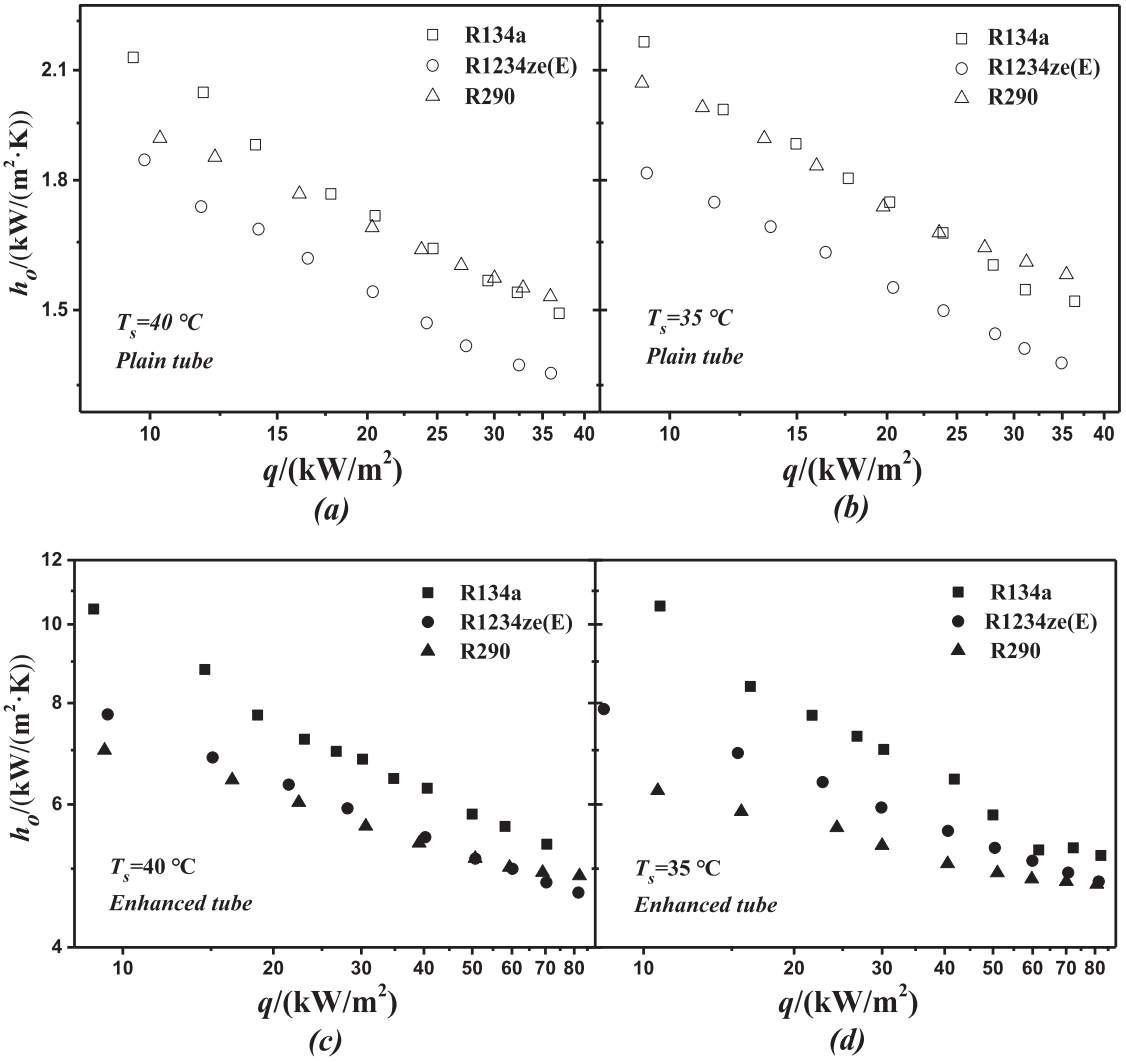

Fig. 7. Condensing heat transfer coefficient versus heat flux at saturation temperature of 40 °C and 35 °C on plain and enhanced tubes.

Table 5
Thermophysical properties of test refrigerants.

	T_s (°C)	P_r (MPa)	r (kJ/kg)	λ (W/m•K)	ρ (kg/m^3)	η (μPa•s)	σ (mN•m)
R134a	35	0.88698	168.18	76.853	1167.5	172	6.7423
	40	0.88698	163.02	74.716	1146.7	161.45	6.1149
R1234ze(E)	35	0.66741	159.02	70.836	1129.3	177.21	7.5777
	40	0.76645	154.8	69.187	1111.5	167	6.956
R290	35	1.2181	316.62	89.024	475.73	87.221	5.2064
	40	1.3696	306.51	86.802	467.07	82.639	5.0918

Fig. 8 compares the condensing heat transfer coefficient of experimental results from literature on low thermal conductivity enhanced tubes. Thermal conductivity of tube materials is shown in Tables 3 and 4 is the detailed parameters of tube shape. The major features are as follows: to begin with, most experimental results of condensing heat transfer coefficient for cupronickel (B10) tube are apparently higher than other tubes. It can be explained from both sides. One is the greater thermal conductivity of cupronickel (B10). The other is highest fin density, optimal fin height and thinnest fin thickness, which is presented in Table 4. Secondly, it is shown in Table 3 that thermal conductivity for stainless steel, aluminum brass (3D fin), cupronickel (B30) and iron cupronickel (3D fin) tubes are ranging from 15.2 to 104.7 W/(m k), but the difference in Fig. 8 is relatively small for condensing heat transfer coefficients on these tubes. Analyzing tube shape of these tubes in Table 4, it was found that fin height and fin density were similar for stainless steel and cupronickel (B30) tubes, while the condensing heat transfer coefficient of cupronickel (B30) was a little bit higher than stainless steel. It indicated that for the tubes with similar fin geometry, the heat transfer coefficient was higher for the tube with higher thermal conductivity. It might be inferred that, for the tubes with lower thermal conductivity, structure of enhanced tube has a little bit less effect on condensing heat transfer coefficient.

As shown in Fig. 9, the experimental results on enhanced tube is also compared with some predicting models for R134a, R1234ze(E) and R290 at saturation temperature of 40 °C. The

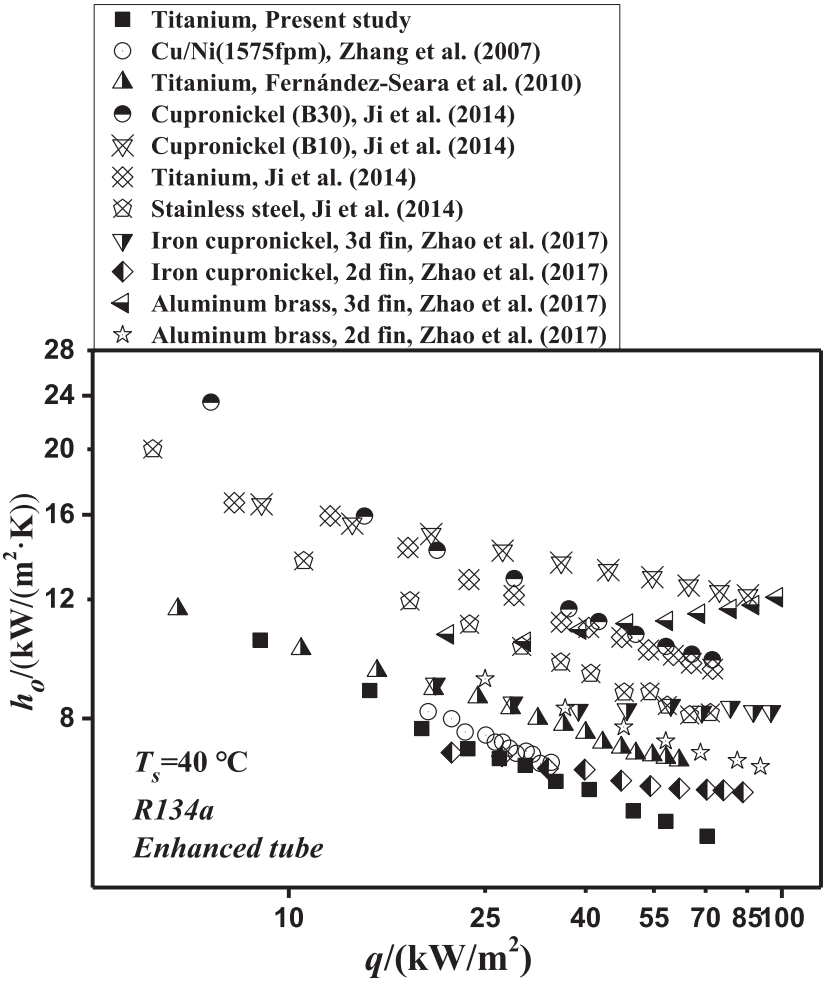

Fig. 8. Comparisons of condensing heat transfer coefficients of experimental results for low thermal conductivity tubes.

prediction models included Beatty and Katz (1948), Owen et al. (1983), Webb et al. (1985), Rose (1994) and Briggs and Rose (1994). It is found in Fig. 9(a)–(b) that prediction models of Beatty–Katz, Owen and Webb underestimate the experimental result, the deviations are ranging from −60.0% to −45.3% for R134a and −62.7% to −35.7% for R1234ze(E), while overestimations of 58.1–63.4% for R134a and 56.0%–70.6% for R1234ze(E) are obtained for Rose model. The model of Briggs–Rose provides a relatively accurate results with deviations of −15.3% ∼ −9.4% for R134a and −25.6% ∼−11.2% for R1234ze(E). For R290 in Fig. 9(c), the deviations are relatively larger. The deviation even reaches −89.6% ∼ −68.9% for the model of Briggs–Rose. The reason was chiefly due to the difference of thermophysical properties for R290, R134a and R1234ze(E), such as latent heat of refrigerant r, liquid refrigerant density ρ and viscosity of refrigerant η (see Table 5).

5.4. Effect of saturation temperature on condensing heat transfer coefficient

For the refrigerant at different saturate temperature, the major difference might be the changes in surface tension and viscosity. The experimental results are showed in Fig. 10 with condensing heat transfer coefficient versus heat flux at different saturation temperature. It can be observed that for R134a and R1234ze(E), the condensing heat transfer coefficients at saturation temperature of 35 °C are mostly similar with that at 40 °C. It is interesting to note that for R290, the condensing heat transfer coefficient for plain tube at saturate temperature of 35 °C is a little bit higher than that for 40 °C. While, for the low-fin enhanced tube, it is just the opposite. The condensing heat transfer coefficient is increasing with increment of saturation temperature.

According to the investigation, the heat transfer coefficient in water side for the tube with low thermal conductivity is almost identical with copper. The thickness of the tube wall plays an important role in the heat transfer. In order to enhance the heat transfer, it should be reduced to the minimum value under the prerequisite of strength and corrosion allowance. The condensing heat transfer coefficient should be higher for tubes with higher thermal conductivity. Fin efficiency is another important factor that have the effect on the condensing heat transfer. For low thermal conductivity tubes, at the same water side velocity, inlet temperature and saturate temperature, the temperature difference of fin roots and vapor should be lower than copper tubes. Although the condensing heat transfer coefficient might be a little bit higher (e.g., $h \propto \Delta t^{-0.25}$), the reduction of temperature difference between the fins and film vapor will reduce the heat transfer rate ($q = h\Delta t \propto \Delta t^{0.75}$). If the heat flux is the same, the average temperature difference between water and refrigerant vapor should be higher than that for copper tubes. It can be assumed that the thermal resistance of shell side, tube side and tube wall comprised one third of the total. Enhance the external, internal and tube wall heat transfer can all have effects on the overall heat transfer performance.

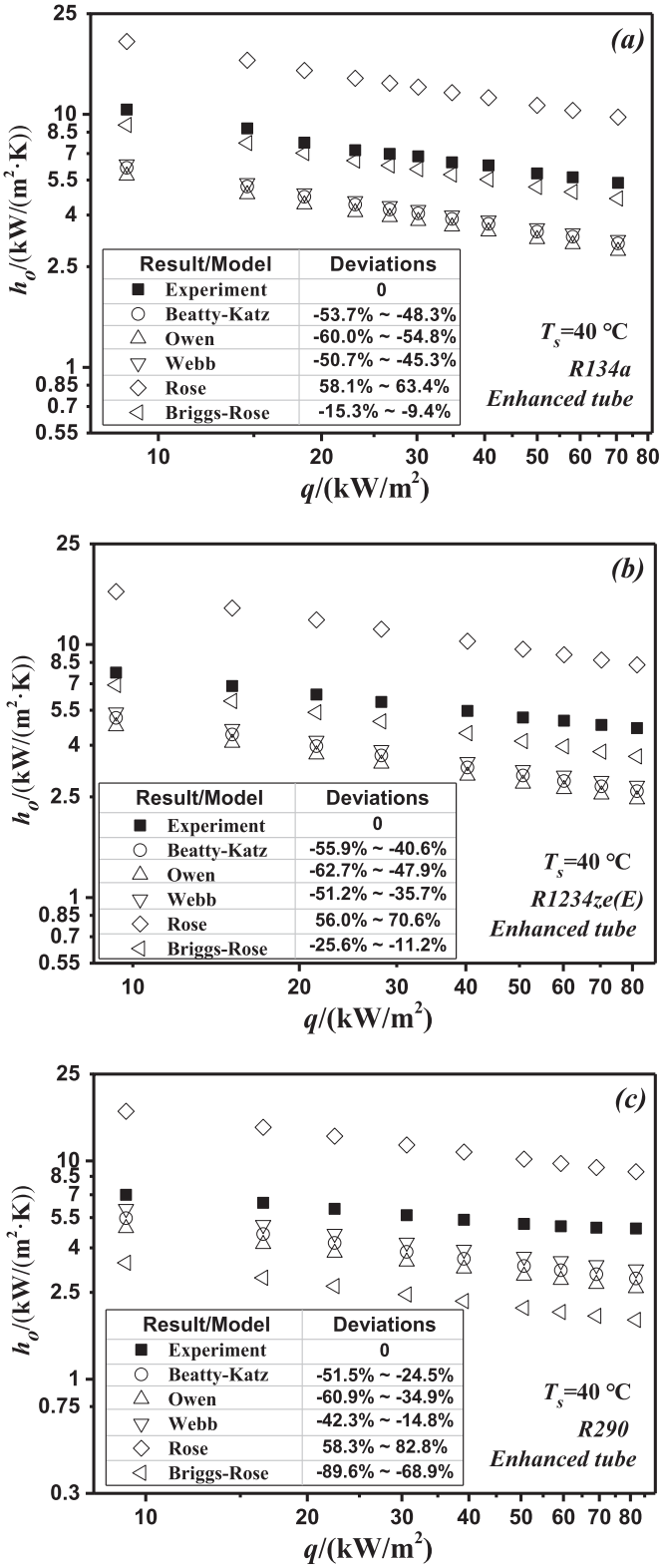

Fig. 9. Comparisons of experimental result and five prediction models for enhanced tube.

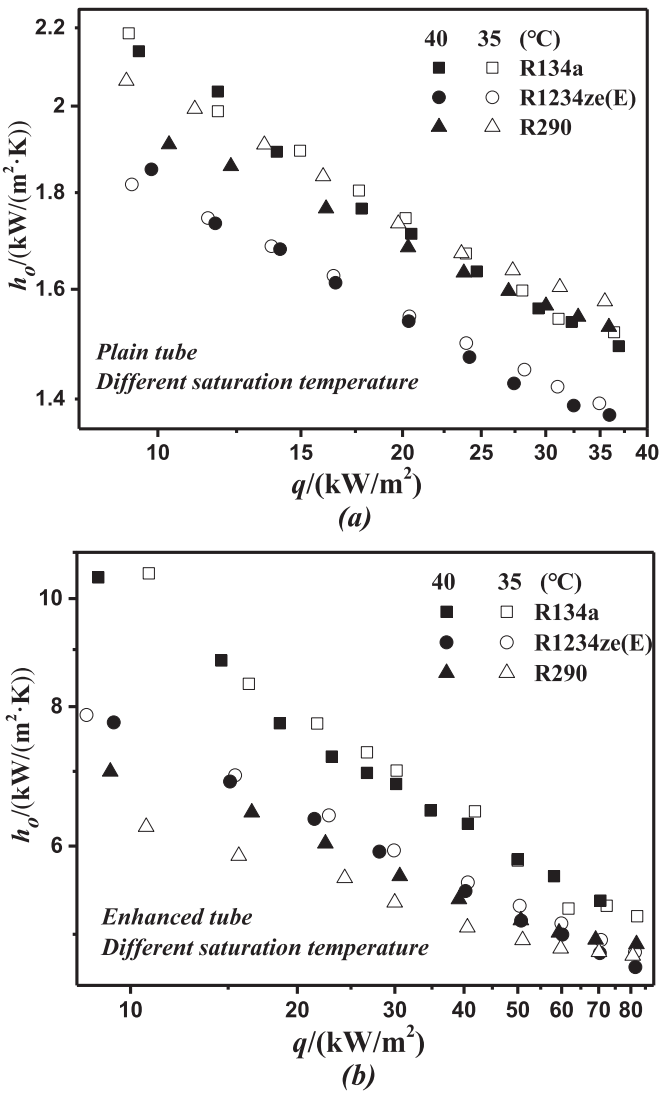

Fig. 10. Effect of saturation temperature on condensing heat transfer coefficients.

6. Conclusions

In this paper, condensation heat transfer of R134a, R1234ze(E) and R290 on plain and enhanced titanium tubes were investigated at saturation temperature of 35 °C and 40 °C. The heat flux was ranging from 8–80 kW/m^2. According to the experimental results, some conclusions can be drawn as follows:

The deviation of experimental result and Nusselt analytical solution on plain tube was within ±12% for R134a, R1234ze(E) and R290. At higher heat flux, the experimental result was a little bit higher than the Nusselt prediction result.

The overall heat transfer coefficient for R1234ze(E) and R290 were both lower than R134a for both plain and enhanced tubes. Heat flux had less effect on the overall heat transfer coefficient of R290 on the enhanced tube.

Condensing heat transfer coefficient of R134a was the largest. For the plain tube, heat transfer coefficient of R290 was very close to R134a. While for enhanced tube, it was the lowest for the three refrigerants.

Five models were used to predict experimental condensing heat transfer coefficients of R134a, R1234ze(E) and R290. Comparisons showed that the model of Briggs–Rose gave a better prediction result for R134a and R1234ze(E), while the model underestimated the experimental result for R290.

The effect of saturate temperature on the condensing heat transfer of R134a, R1234ze(E) was even negligible. While for R290, the condensing heat transfer coefficient was increasing with increment of saturate temperature for enhanced tubes.

Acknowledgment

This work was supported by the National Natural Science Foundation of China (51776160), National Key Research and Development Program of China (2016YFB0601204) and 111 Project (B16038).

References

Al-Badri, A.R., Bär, A., Gotterbarm, A., Rausch, M.H., Fröba, A.P., 2016. The influence of fin structure and fin density on the condensation heat transfer of R134a on single finned tubes and in tube bundles. Int. J. Heat Mass Transf. 100, 582–589.

Al-Badri, A.R., Gebauer, T., Leipertz, A., Fröba, A.P., 2013. Element by element prediction model of condensation heat transfer on a horizontal integral finned tube. Int. J. Heat Mass Transf. 62, 463–472.

Beatty, K.O., Katz, D.L., 1948. Condensation of vapors on outside of finned tubes. Chem. Eng. Prog. 44, 908–914.

Bergman, T.L., 2011. Introduction to Heat Transfer. John Wiley & Sons.

Briggs, A., Rose, J., 1994. Effect of fin efficiency on a model for condensation heat transfer on a horizontal, integral-fin tube. Int. J. Heat Mass Transf. 37, 457–463.

Cheng, B., Tao, W., 1994. Experimental study of R-152a film condensation on single horizontal smooth tube and enhanced tubes. J. Heat Transf. 116, 266–270.

Fernández-Seara, J., Uhía, F.J., Diz, R., Dopazo, A., 2010. Condensation of R-134a on horizontal integral-fin titanium tubes. Appl. Therm. Eng. 30, 295–301.

Gebauer, T., Al-Badri, A.R., Gotterbarm, A., Hajal, J.E., Leipertz, A., Fröba, A.P., 2013. Condensation heat transfer on single horizontal smooth and finned tubes and tube bundles for R134a and propane. Int. J. Heat Mass Transf. 56, 516–524.

Gnielinski, V., 1976. New equations for heat and mass transfer in turbulent pipe and channel flow. Int. Chem. Eng. 16, 359–368.

Ji, W.-T., Li, Z.-Y., Qu, Z.-G., Guo, J.-F., Zhang, D.-C., He, Y.-L., Tao, W.-Q., 2015a. Film condensing heat transfer of R134a on single horizontal tube coated with open cell copper foam. Appl. Therm. Eng. 76, 335–343.

Ji, W.-T., Numata, M., He, Y.-L., Tao, W.-Q., 2015b. Nucleate pool boiling and filmwise condensation heat transfer of R134a on the same horizontal tubes. Int. J. Heat Mass Transf. 86, 744–754.

Ji, W.-T., Zhao, C.-Y., Zhang, D.-C., Li, Z.-Y., He, Y.-L., Tao, W.-Q., 2014. Condensation of R134a outside single horizontal titanium, cupronickel (B10 and B30), stainless steel and copper tubes. Int. J. Heat Mass Transf. 77, 194–201.

Jung, D., Chae, S., Bae, D., Oho, S., 2004. Condensation heat transfer coefficients of flammable refrigerants. Int. J. Refrig. 27, 314–317.

Kline, S.J., 1953. The description of uncertainties in single sample experiments. Mech. Eng. 75, 3–9.

Lienhard, J.H., 2013. A Heat Transfer Textbook. Courier Corporation.

Nagata, R., Kondou, C., Koyama, S., 2016. Comparative assessment of condensation and pool boiling heat transfer on horizontal plain single tubes for R1234ze (E), R1234ze (Z), and R1233zd (E). Int. J. Refrig. 63, 157–170.

Nusselt, W., 1916. Dia Oberflachen condensation des wasserdampfes. Zeitchrift des Vereines deustcher Ingenieure 60, 1645–1648.

Owen, R., Sardesai, R., Smith, R., Lee, W., 1983. Gravity controlled condensation and horizontal low-fin tube, condensers: theory and practice. In: Symposium, pp. 415–428.

Rose, J., 1994. An approximate equation for the vapour-side heat-transfer coefficient for condensation on low-finned tubes. Int. J. Heat Mass Transf. 37, 865–875.

Webb, R., Rudy, T., Kedzierski, M., 1985. Prediction of the condensation coefficient on horizontal integral-fin tubes. J. Heat Transf. 107, 369–376.

Yunus, A.C., Ghajar, A.J., 2007. Transferencia de Calor y Masa, Segunda edición Editorial Mc GrawHill México, México. DF.

Zhang, D.-C., Ji, W.-T., Tao, W.-Q., 2007. Condensation heat transfer of HFC134a on horizontal low thermal conductivity tubes. Int. Commun. Heat Mass Trans. 34 (8), 917–923.

Zhao, C.-Y., Ji, W.-T., Jin, P.-H., Zhong, Y.-J., Tao, W.-Q., 2017. The influence of surface structure and thermal conductivity of the tube on the condensation heat transfer of R134a and R404A over single horizontal enhanced tubes. Appl. Therm. Eng. 125, 1114–1122.